Cell, Vol. 96, 879–891, March 19, 1999, Copyright ©1999 by Cell Press

Transmembrane Structure of an Inwardly Rectifying Potassium Channel

Daniel L. Minor, Jr., Susan J. Masseling, Yuh Nung Jan, and Lily Yeh Jan*
Howard Hughes Medical Institute
Departments of Physiology and Biochemistry
University of California
San Francisco, California 94143-0725

Summary

Inwardly rectifying potassium channels (K_{ir}), comprising four subunits each with two transmembrane domains, M1 and M2, regulate many important physiological processes. We employed a yeast genetic screen to identify functional channels from libraries of K_{ir} 2.1 containing mutagenized M1 or M2 domains. Patterns in the allowed sequences indicate that M1 and M2 are helices. Protein–lipid and protein–water interaction surfaces identified by the patterns were verified by sequence minimization experiments. Second-site suppressor analyses of helix packing indicate that the M2 pore-lining inner helices are surrounded by the M1 lipid-facing outer helices, arranged such that the M1 helices participate in subunit–subunit interactions. This arrangement is distinctly different from the structure of a bacterial potassium channel with the same topology and identifies helix-packing residues as hallmark sequences common to all K_{ir} superfamily members.

Introduction

Inwardly rectifying potassium channels (K_{ir}) are integral membrane proteins that comprise a superfamily of eukaryotic channels responsible for regulating processes that include cell excitability, vascular tone, heart rate, renal salt flow, and insulin release. They have a direct physiological effect on the membrane potential of cells in the brain, vasculature, heart, and pancreas (Hille, 1992; Doupnik et al., 1995; Jan and Jan, 1997; Nichols and Lopatin, 1997). Loss-of-function mutations in various K_{ir} genes result in hypertension, familial hyperinsulinimia, or the elimination of slow inhibitory postsynaptic potentials in central neurons (Simon et al., 1996; Lüscher et al., 1997; Nestorowicz et al., 1997). Under appropriate electrochemical potentials, they conduct more inward than outward potassium current. However, the conditions necessary to drive inward current fluxes are rarely met in animal cells. Thus, despite their name, the principal physiological currents K_{ir} channels conduct are outward potassium currents.

The K_{ir} superfamily comprises at least seven distinct subfamilies that respond to different types of regulation. Members are designated K_{ir} x.y, where "x" designates the subfamily and "y" designates the subtype within the subfamily (Doupnik et al., 1995). K_{ir} channel family subtypes are regulated by a variety of factors. In constitutively active K_{ir} channels like K_{ir} 2.1, the reduction in outward current is mediated by small cytoplasmic molecules like polyamines or magnesium ions that physically plug the conduction pore (Nichols and Lopatin, 1997). In addition to these factors, other subfamily members are regulated by modulators that include G protein $\beta\gamma$ subunits (K_{ir} 3.x), ATP (K_{ir} 1.1, K_{ir} 4.1) or the ATP and ADP concentrations that reflect the metabolic state of the cell (K_{ir} 6.x/sulfonylurea receptor complexes) and the lipid PIP_2 (Doupnik et al., 1995; Wickman and Clapham, 1995; Nichols and Lopatin, 1997; Babenko et al., 1998; Baukrowitz et al., 1998; Huang et al., 1998; Shyng and Nichols, 1998; Sui et al., 1998).

K_{ir} channels have the simplest structural plan of characterized eukaryotic channels. Most K_{ir} channels are tetramers (Yang et al., 1995; Corey et al., 1998; Raab-Graham and Vandenberg, 1998) that are assembled from either identical or nonidentical subunits to make functional channels that are either homomeric or heteromeric. This combinatorial diversity in assembly leads to a great deal of functional diversity. Each subunit has two transmembrane segments (M1 and M2), a region responsible for monovalent cation selectivity (P region), and N- and C-terminal cytoplasmic domains (Figure 1A). The P region is located in the membrane domain and contains the signature tripeptide sequence G(Y/F)G that is common to all potassium channels (Heginbotham et al., 1994). The two transmembrane segments M1 and M2, which comprise the remainder of the membrane domain, are similar among K_{ir} channels but are only distantly related to other potassium channels.

Obtaining high-resolution structural information for eukaryotic membrane proteins remains a difficult problem. However, the hydrophobic nature of the cell membrane seems to restrict transmembrane protein structure to relatively regular architectures such as helical bundles or β barrels (Lemmon and Engelman, 1994; von Heijne, 1997). Consequently, techniques that can identify periodicities characteristic for secondary structure types like mutagenesis (Lemmon et al., 1992) or site-directed spin labeling techniques (Hubbell et al., 1998; Perozo et al., 1998) can provide useful structural information for transmembrane protein domains at the level of the backbone fold. To this end, we used rescue of a potassium transport–deficient strain of yeast, SGY1528 (Δ*trk1*, Δ*trk2*) (Tang et al., 1995), by functional K_{ir} 2.1 channels encoded in randomized libraries, to probe the local environments of amino acids in the transmembrane segments of K_{ir} 2.1.

Many sequences in our libraries encode functional channels. Within these sequences, clear position-specific preferences are observed with respect to side chain shape and chemistry. The patterns of allowed amino acid substitutions suggest that both M1 and M2 transmembrane segments are helical and identify protein–protein, protein–lipid, and protein–water interaction surfaces. A structural model for the arrangement of the transmembrane segments was developed and tested by

*To whom correspondence should be addressed (e-mail: gkw@itsa.ucsf.edu).

A

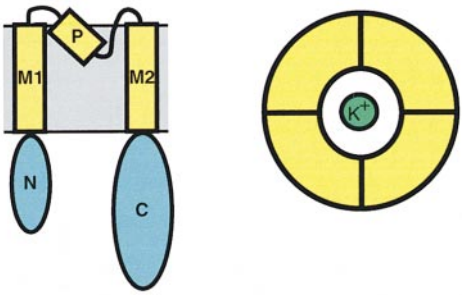

B

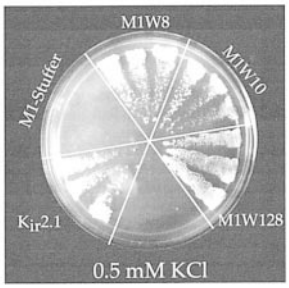

C

	M1 Library	M2 Library
Complexity	1.0×10^6	8.6×10^5
Screened	7.0×10^4	4.3×10^4
Winners	1.0×10^4	9.8×10^3
% Winners	15%	22%
Background	0.3%	0.3%
Amino acid changes/sequence (Unselected)	4.5	4.2
Amino acid changes/sequence (Winners)	2.6	3.0

Figure 1. Membrane-Spanning Topology of K_{ir} 2.1 and Selection for Functional Channels

(A) Cartoon schematics of K_{ir} channel structure. The membrane domains are colored yellow and the cytoplasmic domains blue. The left-hand cartoon represents a single subunit. M1, M2, and P indicate the two transmembrane segments and the selectivity filter, respectively. The right-hand cartoon represents an extracellular view of an assembled tetrameric K_{ir} channel. The green sphere represents a potassium ion.

(B) Rescue of the potassium transport–deficient yeast strain SGY1528 under selective conditions. Yeast-bearing plasmids expressing K_{ir} 2.1 and K_{ir} 2.1 mutants are indicated. M1-stuffer is a nonfunctional K_{ir} 2.1 mutant where the M1 domain is replaced with 300 amino acids from a soluble protein. Functional K_{ir} 2.1 mutants are as follows: M1W8: I87N, F88I, V93G, F98L, G100A; M1W10: F88L, A91V, L94V, L97C, G100A; M1W128: F88V, C89G, C101F, V102A.

(C) Selection of functional K_{ir} 2.1 channels from randomized libraries. Library sizes, numbers of yeast screened in each library, the percentage of surviving yeast colonies, "winners," and the average number of observed amino acid changes per sequence are indicated. Background was determined by transforming nonfunctional K_{ir} 2.1-stuffer (see Experimental Procedures) clones in parallel with the libraries. In the M1 library, 314 amino acid changes were observed in 122 independent sequences, and in the M2 library, 369 amino acid changes were observed in 123 independent sequences.

sequence minimization experiments as well as second-site suppressor experiments, to probe helix–helix contacts. Taken together, the data indicate that the transmembrane structure of K_{ir} channels is a helical bundle where M1 and M2 form the outer and inner helices, respectively.

Comparison of the structural constraints derived here with the X-ray crystallographic structure of a bacterial potassium channel with the same topology (Doyle et al., 1998) indicates that these two types of channels have distinct differences in quaternary structure, although the tertiary structure between M1 and M2 helices within a single subunit is similar. The patterns of allowed amino acid substitutions observed in our selection experiments identify sequence features that are hallmarks of the K_{ir} superfamily and absent in other potassium channel types. Together, the results presented here strongly suggest that K_{ir} channels form a structurally distinct class of potassium channels with respect to transmembrane structure.

Results

Selection for Functional K_{ir} 2.1 Channels

Rescue of the growth of the potassium transport–deficient yeast SGY1528 (Tang et al., 1995) under selective conditions identified functional K_{ir} 2.1 channels from libraries in which either of the transmembrane domains were subjected to random mutagenesis (Figure 1B). The gene segments encoding the transmembrane domains of K_{ir} 2.1 (Kubo et al., 1993) were replaced with synthetic oligonucleotide cassettes bearing on average five codon changes per cassette to create libraries of channels with transmembrane domains with high amino acid substitution rates. For both libraries, 50 unselected clones were sequenced to verify that all positions had similar rates of mutation. The M1 and M2 libraries encode a large number of functional channels (Figure 1C), suggesting that both transmembrane segments are very tolerant to amino acid changes, a result observed for other membrane proteins (Wen et al., 1996; Kaback et al., 1997). However, in contrast to many membrane proteins, the high variability is position specific. Both M1 and M2 have many side chains that have restricted requirements for both shape and chemistry (Figure 2; Table 1) reminiscent of patterns observed in soluble proteins (Bowie et al., 1990) and suggesting that well-defined packing interactions are present. Importantly, electrophysiological examination of positive clones from the selection experiments demonstrates that channels that rescue yeast are functional K_{ir} channels with wild-type properties (Figure 3). The selection seems to be very stringent, as mutations that drastically reduce but do not abolish channel activity in *Xenopus* oocyte assays do not rescue (data not shown).

The transmembrane positions were classified as tolerant (green), moderately tolerant (blue), or restricted (red) with respect to the number and type of substitutions allowed (Figure 2). The assignment of tolerant and restricted positions was fairly straightforward. The semitolerant designation denotes positions that vary at a low frequency to a generally restricted class of residues with similar properties to the native residue such as β branching, hydrophobicity, or volume. The assignment of residues into the semitolerant class is somewhat subjective but not critical to the subsequent structural interpretation of the data. We assume that most amino acid

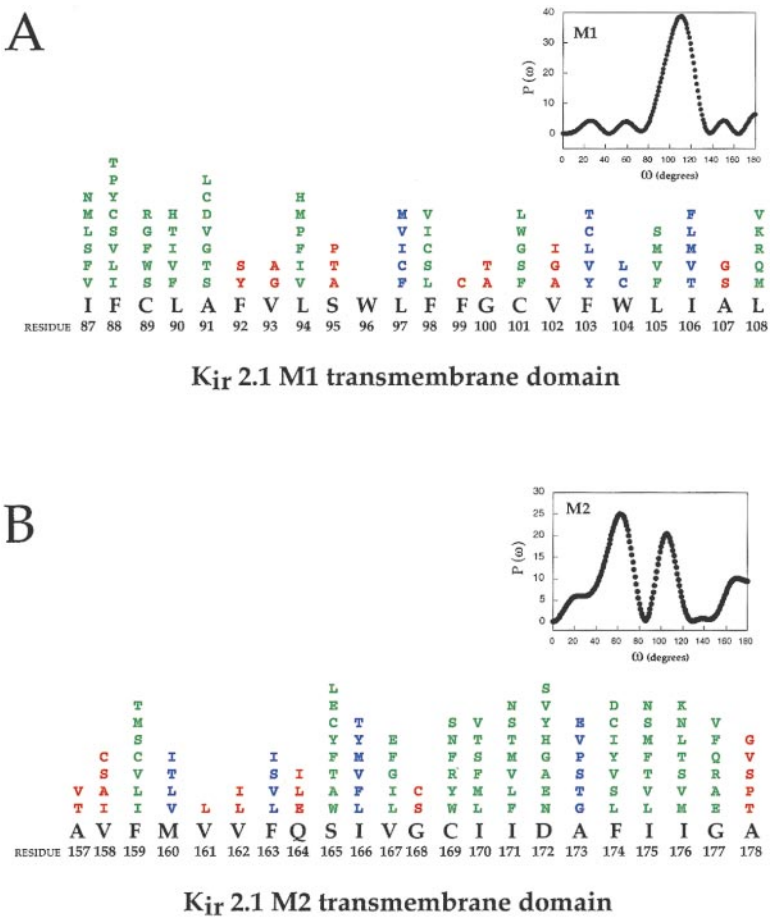

Figure 2. Functional Substitutions and Periodicity Analysis

(A) Allowed amino acid changes in the M1 domain of K_{ir} 2.1. The wild-type residue is shown in black. Changes are arranged with the most frequently observed amino acid change placed closest to the wild-type sequence and the least frequent at the top of the column. Positions are color coded: green, tolerant; blue, semitolerant; red, restricted. Classifications were assigned on a position by position basis by considering the nature of the allowed changes relative to the wild-type residue and the frequency of change. Total changes for amino acids at each position are given in Table 1. Inset shows the power spectra calculated as described (Cornette et al., 1987; Rees et al., 1990).

(B) Allowed amino acid changes in the M2 domain of K_{ir} 2.1. Sequences are depicted as in (A).

changes in the functional sequences are not correlated. No obvious covariation patterns could be discerned for changes at restricted or semitolerant positions.

Structural Analysis of Sequence Patterns

Regular secondary structures in anisotropic environments can be identified using discrete Fourier transform techniques to evaluate periodic variation in parameters that are a function of residue position, such as side chain variability, hydrophobicity, or accessibility (Cornette et al., 1987; Rees et al., 1990). We examined the variation of allowed amino acid substitutions in the M1 and M2 transmembrane segments for patterns characteristic of secondary structure using these methods. This evaluation is independent of the color-coded classification scheme, as the parameter that is evaluated is simply the total number of unique amino acid changes allowed at each position. The power spectrum of the amino acid variability in M1 contains a single peak at $\omega = 110°$ (Figure 2A inset), a frequency in the range characteristic of α helices. The power spectrum of the amino acid variability in M2 is more complex, containing a strong peak at the helical hallmark frequency $\omega = 105°$ (Figure 2B inset) in addition to a larger lower frequency peak. This feature is commonly observed for helices in less anisotropic environments (Cornette et al., 1987; Perozo et al., 1998). The frequencies observed for M1 and M2 are within the range seen for α helices (Cornette et al., 1987) and are frequencies that are characteristic of α-helical structure with a heptad-type repeat ($\omega = 103°$ for a strict heptad repeat of 3.5 amino acids/turn).

In an α helix with a heptad repeat, residues on the same face of the helix occur with a 3–4 spacing in the primary sequence (Cohen and Parry, 1990). The most tolerant positions in M1 occur with this spacing and were placed at the "a" and "d" positions of a heptad helical wheel diagram (Figure 4A) (Cohen and Parry, 1990). This reveals a clear segregation of residue types onto different helical faces. Restricted positions fall on one face of the M1 helix (positions "b," "c," "e," and "f") while the tolerant positions fall on the opposite face (positions "a," "d," and "g"). Residues on the restricted face include strongly conserved residues among K_{ir} sequences: F92, S95, W96, F99, G100, and A107. Lipid-facing residues in membrane proteins show high variability for hydrophobic residues, while the side chain properties of buried interior positions are restricted (Rees et al., 1990; Donnelly et al., 1993; Wallin et al., 1997). Our data suggest that positions "a," "d," and possibly "g" form the protein–lipid interface of M1, whereas positions "b," "c," "e," and "f" present a surface for protein–protein interactions. Therefore, we designate M1 as the "outer helix" located between the lipids and the protein interior.

M2 residues tolerating positive charges and many of the most drastic changes observed (cf. S165W/E,

Table 1. Observed Substitutions in M1 and M2 of K_{ir} 2.1

M1																
I	87	V	(4)	F	(2)	S	(2)	L	(1)	M	(1)	N	(1)			11
F	88	I	(15)	L	(13)	V	(9)	S	(6)	C	(5)	Y	(3)	P	(1)	T (1)	53
C	89	S	(10)	W	(4)	F	(3)	G	(2)	R	(1)					20
L	90	F	(3)	V	(2)	I	(1)	T	(1)	H	(1)					8
A	91	S	(8)	T	(8)	G	(4)	V	(4)	D	(2)	C	(1)	L	(1)	28
F	92	Y	(4)	S	(3)											7
V	93	G	(2)	A	(2)											4
L	94	V	(8)	I	(3)	F	(2)	P	(2)	M	(1)	H	(1)			17
S	95	A	(2)	T	(1)	P	(1)									4
W	96															0
L	97	F	(2)	C	(1)	I	(1)	V	(1)	M	(1)					6
F	98	L	(21)	S	(13)	C	(7)	I	(5)	V	(4)					50
F	99	C	(1)													1
G	100	A	(8)	T	(1)											9
C	101	F	(17)	S	(6)	G	(2)	W	(2)	L	(1)					28
V	102	A	(4)	G	(2)	I	(1)									7
F	103	Y	(7)	V	(4)	L	(1)	C	(1)	T	(1)					14
W	104	C	(5)	L	(3)											8
L	105	F	(6)	V	(4)	M	(3)	S	(1)							14
I	106	T	(4)	V	(3)	M	(2)	L	(1)	F	(1)					11
A	107	G	(1)	S	(1)											2
L	108	M	(4)	Q	(3)	R	(3)	K	(1)	V	(1)					12
M2																
A	157	T	(1)	V	(1)											2
V	158	I	(7)	A	(1)	S	(1)	C	(1)							10
F	159	I	(16)	L	(10)	V	(4)	C	(4)	S	(3)	M	(1)	T	(1)	39
M	160	V	(5)	L	(3)	T	(3)	I	(1)							12
V	161	L	(2)													2
V	162	L	(4)	I	(2)											6
F	163	L	(6)	V	(5)	S	(4)	I	(3)							18
Q	164	E	(7)	L	(1)	I	(1)									9
S	165	W	(6)	A	(4)	T	(4)	F	(2)	Y	(2)	C	(1)	E	(1)	L (1)	21
I	166	L	(10)	F	(6)	V	(4)	M	(4)	Y	(1)	T	(1)			26
V	167	L	(15)	I	(3)	G	(3)	F	(1)	E	(1)					23
G	168	S	(3)	C	(2)											5
C	169	W	(4)	Y	(4)	R	(4)	F	(3)	S	(2)	N	(1)			18
I	170	L	(4)	M	(3)	F	(2)	S	(2)	T	(2)	V	(1)			14
I	171	F	(4)	L	(3)	M	(2)	T	(2)	S	(1)	N	(1)			16
D	172	N	(7)	E	(5)	A	(2)	G	(2)	H	(2)	Y	(1)	V	(3)	S (1)	21
A	173	G	(5)	T	(5)	S	(3)	P	(2)	V	(1)	E	(1)			17
F	174	L	(6)	S	(3)	V	(2)	Y	(1)	I	(1)	C	(1)	D	(1)	15
I	175	L	(8)	V	(6)	T	(6)	S	(4)	F	(3)	M	(3)	N	(1)	31
I	176	M	(7)	V	(6)	S	(6)	T	(5)	L	(3)	N	(1)	K	(1)	29
G	177	E	(7)	A	(3)	R	(2)	Q	(1)	F	(1)	V	(1)			15
A	178	T	(9)	P	(5)	S	(3)	V	(3)	G	(1)					21

The first column indicates the wild-type residue. Subsequent columns indicate observed amino acid substitutions in functional channels; the number of times the change was observed is given in parentheses. The last column indicates the total number of changes observed at each position. The number of total substitutions per M1 or M2 sequence is listed below as number of changes (observed independent sequences): M1: 1(28), 2(37), 3(30), 4(17), 5(6), 6(4); M2: 1(20), 2(29), 3(31), 4(23), 5(14), 6(4), 7(2).

C169W/R, D172Y/H, I176N/K) similarly occur with a 3–4 spacing. These were placed at the "a" and "d" positions of a heptad wheel diagram (Figure 4B). As a result, one face of the helix contains the highly variable residues, while another (positions "c" and "g") contains restricted residues that are highly conserved among K_{ir} channels: A157, V161, Q164, and G168. One of the residues on the highly variable face, residue 172, has been shown to influence K_{ir} channel rectification properties through interactions with a pore-blocking magnesium ion (Lu and MacKinnon, 1994; Stanfield et al., 1994; Wible et al., 1994; Reuveney et al., 1996). This, together with the high variability and tolerance for charged residues at positions on the face containing residues 165, 169, 172, and 176, suggests that these positions are exposed to an aqueous environment in the pore of the channel. Thus, we designate M2 as the pore-lining "inner helix."

Sequence Minimization

We used a sequence minimization approach to test the assignment of the lipid-facing and pore-facing residues. Residues suspected of participating in these interfaces were simultaneously altered to probe the general properties of the environment of a given face of the helix. For the predicted lipid-facing residues of M1, we made K_{ir} 2.1 channels where the M1 "a" and "d" positions—

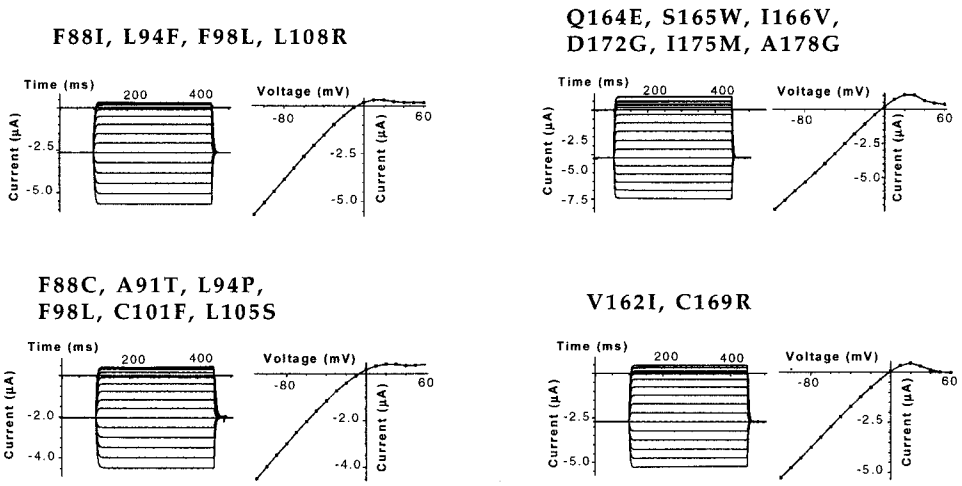

Figure 3. K_{ir} 2.1 Mutants that Rescue Yeast Are Functional Inward Rectifiers

Two-electrode voltage clamp recordings from *Xenopus* oocytes expressing M1 and M2 mutants isolated from the screen. Amino acid changes within each mutant are indicated. Diplayed currents are the difference between 90 K and 90 Na solutions.

seven residues in total—or the M1 "a," "d," and "g" positions—ten residues in total—were changed wholesale either to the hydrophobic residues alanine, leucine, or phenylalanine or to the hydrophilic residue serine (M1ad–Xaa_7 and M1adg–Xaa_{10}, respectively). Two-electrode voltage clamp recordings from *Xenopus* oocytes demonstrate that M1ad–Ala_7, –Leu_7, and –Phe_7 and M1adg–Ala_{10}, –Leu_{10}, and Phe_{10} form functional channels

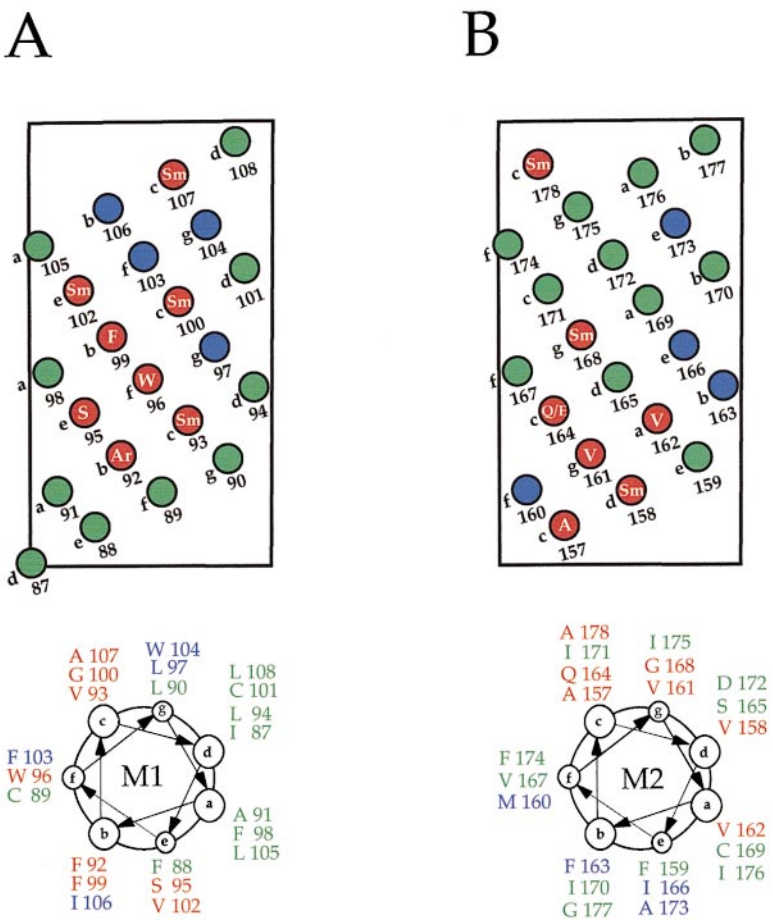

Figure 4. Helical Diagrams of K_{ir} 2.1 Amino Acid Tolerance Patterns

Helical wheel and net diagrams of (A) M1 and (B) M2. The principal side chain types found at the restricted positions are indicated and are as follows: M1 92, aromatic (Ar); 93, small (Sm); 95, Sm, hydroxyl containing (S); 96, tryptophan (W); 99, phenylalanine (F); 100, Sm; 102, Sm; 107, Sm; M2 157, alanine (A); 158, Sm; 161, valine (V) ; 162, V; 164, glutamine/glutamate (Q/E); 168, Sm; 178, Sm. Helical wheels depict the residue number and wild-type residue.

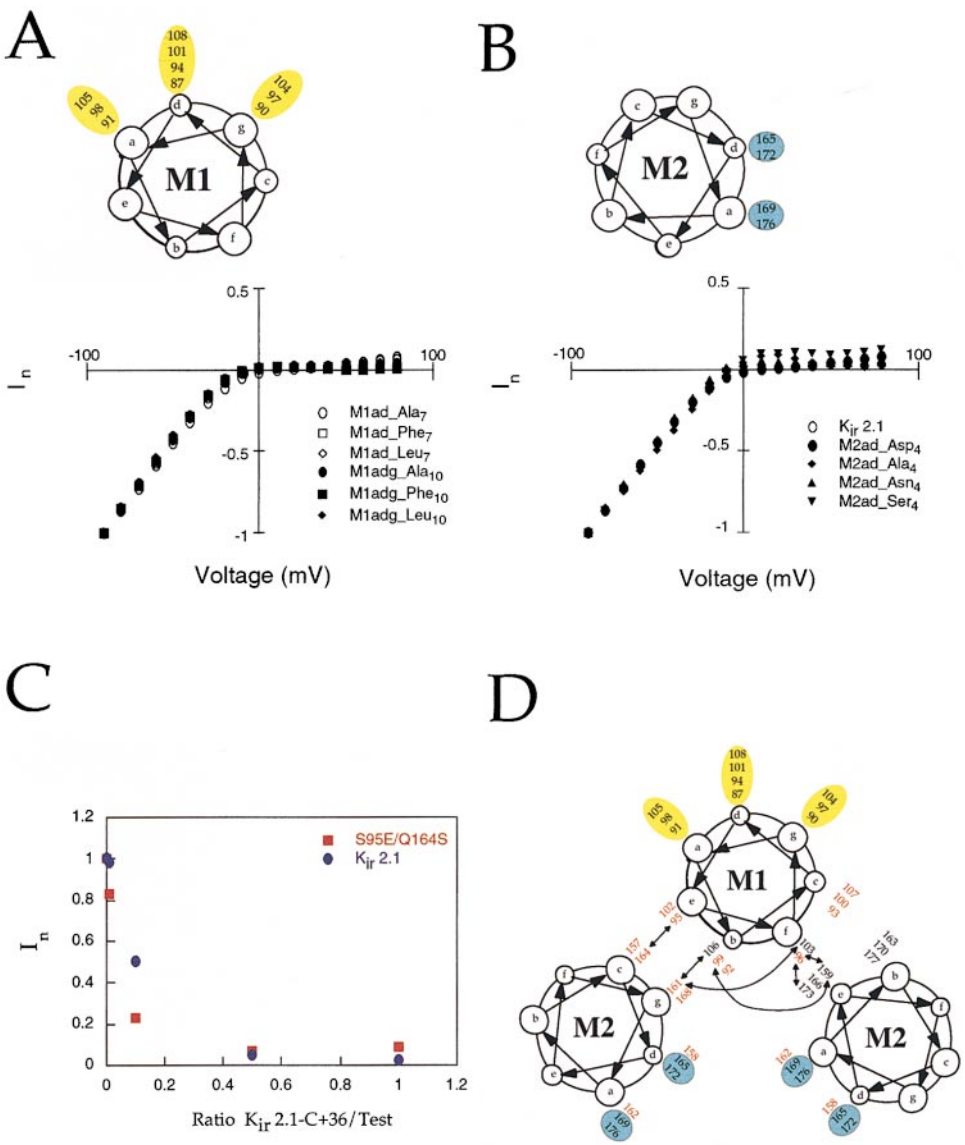

Figure 5. Sequence Minimization, Assembly, and Second-Site Suppressor Experiments

(A) Normalized I–V relationships for M1ad–Xaa$_7$ and M1adg–Xaa$_{10}$ channels. The inset shows a helical wheel diagram with the positions of the M1 helix that were changed highlighted in yellow.

(B) Normalized I–V relationships for M2ad–Xaa$_4$ channels. The inset shows a helical wheel diagram with the positions of the M2 helix that were changed highlighted in blue. Recordings were made from *Xenopus* oocytes expressing the mutant channels and represent the difference between currents recorded in 90 K and 90 Na solutions. Inward potassium currents in (A) and (B) were normalized to the value at −90 mV. The current amplitudes ranged from 1–10 μA.

(C) Interaction assay for the hydrogen bond reversal mutant S95E/Q164S, or wild-type K_{ir} 2.1, with wild-type K_{ir} 2.1-C+36 channels bearing an ER retention signal. Normalized inward potassium-selective current from *Xenopus* oocytes is plotted versus the ratio of K_{ir} 2.1-C+36/test RNA for K_{ir} 2.1 or S95E/Q164S injected (see Experimental Procedures).

(D) Second-site suppressor interactions and sequence-minimized positions. Arrows indicate the positions of the suppressor mutations relative to the position of the nonfunctional mutant they suppress. The mutation and its suppressors were as follows: W96A was suppressed by F159I/A173P or F159V/A173P; F99A was suppressed by F159I; Q164S was suppressed by S95E; and V161W was suppressed by F103Y/I106N. The vertical positions of the mutant relative to the suppressor along the helical axes are consistent with an antiparallel packing arrangement. Positions of the lipid-facing residues are highlighted in yellow; those of the pore-lining residues are highlighted in blue. Restricted positions from the selection experiments are indicated in red. For simplicity, only the relevant residue numbers are displayed.

(Figure 5A). No detectable currents were measured from the M1ad–Ser$_7$ channel. These results support the idea that the residues at "a," "d," and "g" in M1 comprise a protein–lipid interface, as the only necessary requirement is side chain hydrophobicity, not shape or size.

Similarly, we replaced the putative pore-lining residues of M2 (residues 165, 169, 172, and 176) simultaneously with either alanine, serine, asparagine, or aspartate (designated M2ad–Xaa$_4$). M2ad–Ala$_4$, –Ser$_4$, –Asn$_4$, and –Asp$_4$ form functional channels in *Xenopus* oocytes,

Table 2. Tests of the M1/M2 Interhelix Hydrogen Bond

Residue 95	Residue 164	Rescue?
S	Q	Yes
S	E	Yes
S	N	No
S	D	No
S	A	No
S	S	No
E	S	Yes
Q	S	No
D	S	No
A	A	No

Explict hydrogen bonding pairs were examined to assess the structural requirements of the interaction between residues 95 and 164. Results of rescue of SGY1528 under selective conditions, 0.5 mM KCl (see Experimental Procedures), are indicated. Functional channels with nonhydrogen bonding mutations at positions S95 and Q164 were observed rarely in selection from the M1 and M2 libraries. These changes occurred in concert with a number of other mutations. There was one exception, S95P, which was isolated as a single amino acid change. The additional mutations in channels where 95 and 164 were nonhydrogen bonding residues are: C89W, L90F, L94I, S95A, F98S, V102A; F88S, V93A, S95A; V158I, F163L, Q164L, I171F, I176S; and Q164I, G168C, C169S, D172E, F174D, G177R. The change Q164L did not rescue when tested as a single point mutant.

as assessed by two-electrode voltage clamp measurements (Figure 5B). These data strongly suggest that residues 165, 169, 172, and 176 face a hydrophilic environment. Taken together, the minimization experiments support the assignments of M1 and M2 as the outer and inner helices, respectively.

Helical Arrangement

Second-site suppressor experiments were used to map residues involved in interhelix contacts. In these experiments, changes in side chain shape or chemistry that disrupted function were made at conserved positions in the M1/M2 interfaces and screened against libraries of the other helix of the pair. For example, S95 and Q164 are highly conserved in our selection experiments and among all K_{ir} sequences but not in other potassium channel types. We hypothesized that these residues might participate in a membrane-embedded interhelix hydrogen bond. To test this, the mutant Q164S, a nonfunctional mutant that shortens the side chain of one of the proposed hydrogen bonding partners but preserves the hydrogen bonding potential, was screened against a directed library where only residue 95 was randomized. Selection experiments identified a single change, S95E, that restored channel function. This change effectively reverses the positions of the hydrogen bonding partners. We explicitly examined other possible hydrogen bonding pairs at these positions (Table 2). Only combinations that preserve hydrogen bonding potential as well as total side chain length result in functional channels. Specific buried polar interactions have been observed in other membrane proteins (Bargmann and Weinberg, 1988; Lemmon and Engelman, 1992; Sahin-Tóth et al., 1992; Smith et al., 1996) and in helical bundles (Lumb and Kim, 1995), where they play important roles in folding, helix association, and the establishment of specific structure. Our data suggest that the S95/Q164 hydrogen bond may play such a role and can be considered a structural hallmark of K_{ir} channels.

A subunit interaction assay was used to assess whether the S95/Q164 hydrogen bond occurs between M1 and M2 in an inter- or intrasubunit manner. Coexpression in *Xenopus* oocytes of a wild-type K_{ir} 2.1 subunit with a K_{ir} 2.1 subunit modified with a C-terminal endoplasmic reticulum (ER) retention/retrieval signal, K_{ir} 2.1-C+36 (Zerangue et al., in press), led to a reduction in the amount of inward current due to ER retention/retrieval of coassembled channels (Figure 5C). Coexpression of K_{ir} 2.1-C+36 and the hydrogen bond reversal mutant S95E/Q164S led to a similar reduction in current, indicating that the S95E/Q164S mutant can coassemble with the wild-type subunit. Homomeric channels bearing S95/Q164S or S95E/Q164 pairs in the same polypeptide chain are not functional, and S95/Q164S subunits bearing the retention signal were ineffective at reducing current from wild-type subunits (data not shown). If the hydrogen bond interaction occurred between subunits, complexes of S95E/Q164S-K_{ir} 2.1-C+36 subunits would contain nonfunctional pairings. Hence, it would be difficult to explain the compatibility of the hydrogen bond reversal mutant but not the single mutant S95/Q164S with the wild-type subunit, unless the hydrogen bond occurs between residues 95 and 164 from the same subunit.

Both S95/E164 and E95/S164 hydrogen bond pairings make homomeric functional channels when the pair occurs in each polypeptide chain of the homomeric channel (Table 2). If the hydrogen bond interaction occurred in an intersubunit fashion, heteromeric complexes of S95/Q164S and S95E/Q164E subunits would have the S95–E164 and E95–S164 functional pairs. However, coexpression of subunits containing S95/Q164S and S95E/Q164E pairs did not result in measurable current. These observations further support the idea that the hydrogen bond pairing occurs between residues within a single subunit.

To obtain more information about M1/M2 contacts, other suppressors were obtained for nonfunctional mutants with changes at M1- or M2-restricted positions. The changes W96A, F99A, and V161W were rescued by F159I/A173P or F159V/A173P, F159I, and F103Y/I106N, respectively. Together, the positions of suppressors that restore function to other nonfunctional mutants suggest that each M1 helix interacts with two M2 helices (Figure 5D), one from its own subunit via the interface containing the S95/Q164 hydrogen bond and one from the neighboring subunit. Since the open probability for K_{ir} 2.1 is very near 1 at negative potentials (Kubo et al., 1993) and the selection experiments require functional open channels, this arrangement most likely reflects the open state of a K_{ir} channel. This arrangement of transmembrane helices is distinctly different from that seen in the bacterial potassium channel KcsA, which has the same transmembrane topology.

Structural Comparison with a Bacterial Potassium Channel

Recently, the high-resolution structure of a bacterial potassium channel with the same topology as K_{ir} channels

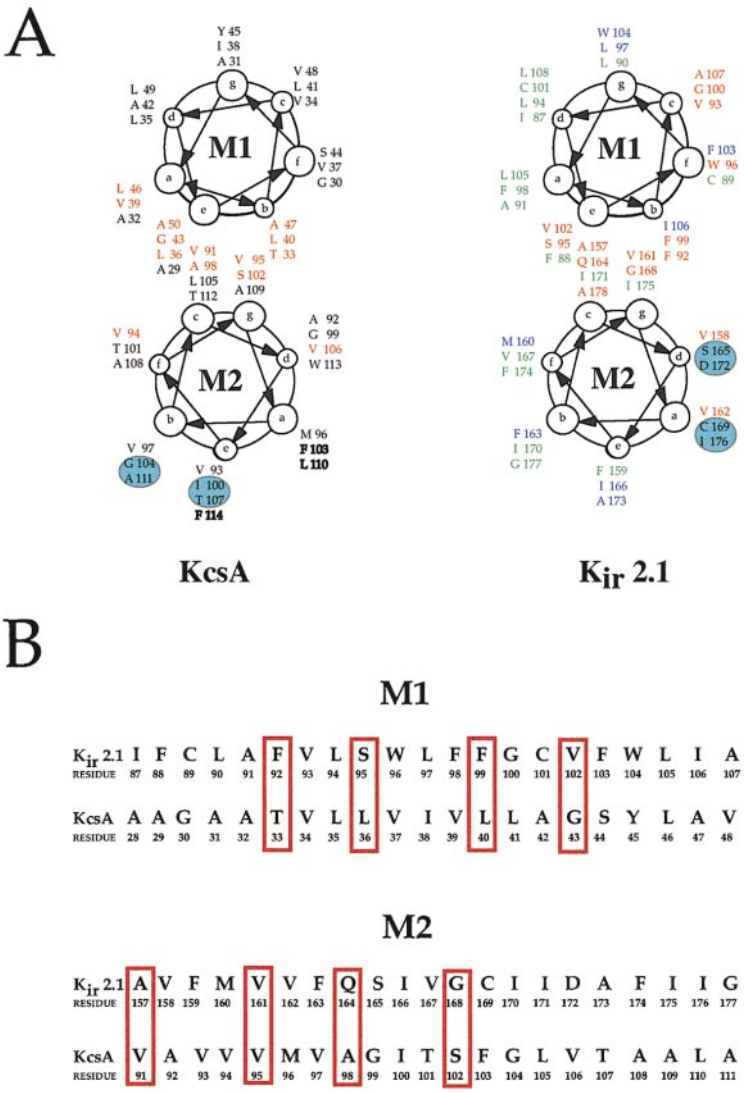

Figure 6. Structural Comparison with the KcsA Bacterial Potassium Channel

(A) Helical wheel diagrams depicting intrasubunit M1/M2 interactions in KcsA and K_{ir} 2.1. M1/M2 KcsA residues that make helix–helix interactions are indicated in red. Nearest-neighbor contacts were identified using a contact analysis program (Oas and Kim, 1988) and were defined as any atom pair with a center to center distance less than or equal to 150% of the sum of the van der Waals (vdW) radii. Invariant K_{ir} 2.1 residues are indicated in red; colors are as in Figure 2. The diagram gives the view from the extracellular side. Pore residues are surrounded by a blue circle. KcsA residues F103, L110, and F114 involved in M2–M2 subunit–subunit interactions are indicated in bold. Residue contacts between M1 and M2 in KcsA were as follows: $0 \leq$ vdW radii $\leq 110\%$: 36–98, 36–102, 40–95, 43–91, 47–91, 50–98; $110\% \leq$ vdW radii $\leq 150\%$: 33–102, 36–95, 39–94, 43–95, 50–91, 46–91, 46–98, and 33–106. The residues in M1 and M2 that make the closest interhelix contacts, $0 \leq$ vdW radii $\leq 110\%$, occur with a 3–4 repeat.

(B) Sequence alignment based on structural analysis of KcsA and mutational analysis of K_{ir} 2.1. Equivalent positions in the 3–4 heptad repeats are surrounded by a red box.

was solved by X-ray diffraction methods (Doyle et al., 1998). In order to compare the structural constraints derived for K_{ir} channels with the KcsA structure, we examined the nearest-neighbor side chain–side chain contacts (Oas and Kim, 1988) in KcsA. This analysis shows that the M1 and M2 helices of KcsA are organized as a pair of antiparallel coils in which each M1 helix only contacts M2 from its own subunit. The principal M1/M2 interface residues occur with a 3–4 heptad repeat (Figure 6A; also see legend). The sequence identity between the transmembrane segments of K_{ir} 2.1 and KcsA is very low. In order to align the sequences, we matched the heptad repeats that comprise the M1/M2 intrasubunit interface (Figure 6B). This results in an alignment that is different from the previously published alignments based on sequence comparison alone (Schrempf et al., 1995; Doyle et al., 1998).

Alignment based on structural constraints indicates that the positions of the interactions between M1 and M2 are conserved in both channel structures, although the exact chemical nature of the side chains in the interface is not similar. For instance, the S95/Q164 hydrogen bond pair corresponds to KcsA L36/A98, two residues in intimate contact with each other across the M1/M2 interface. Structural correspondence also seems to exist between the K_{ir} 2.1 invariant residues V158 and V162 and KcsA M2 residues A92 and M96 that make major contacts to the pore helix, a short helix between M1 and M2 with its carboxy terminal aimed at the ion conductance pathway (Doyle et al., 1998).

There is a poor structural correspondence between K_{ir} 2.1 and KcsA in the residues at the M2/M2 intersubunit interface and the pore-lining residues. Principally, residues that make substantial intersubunit contacts in KcsA, M2 residues F103 and L110, correspond to two positions that show extreme variability in K_{ir} 2.1, 169 and 176. Furthermore, the strong conservation of W96 and G100 in our selection experiments and in all K_{ir} channels cannot be interpreted in light of the KcsA structure, since the corresponding positions (KcsA V37 and L41) have few interactions with other parts of the protein.

Constraints derived from our mutagenesis data suggest that although some basic tertiary structural similarity exists between KcsA and K_{ir} 2.1, the transmembrane

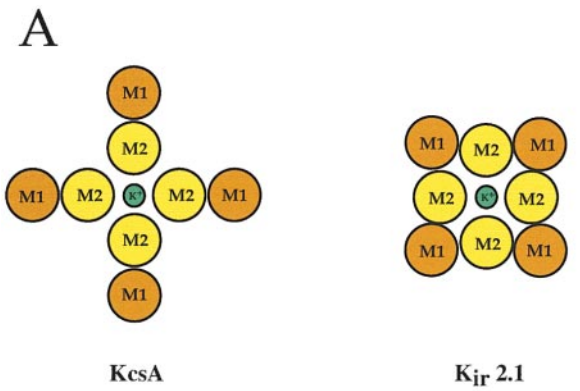

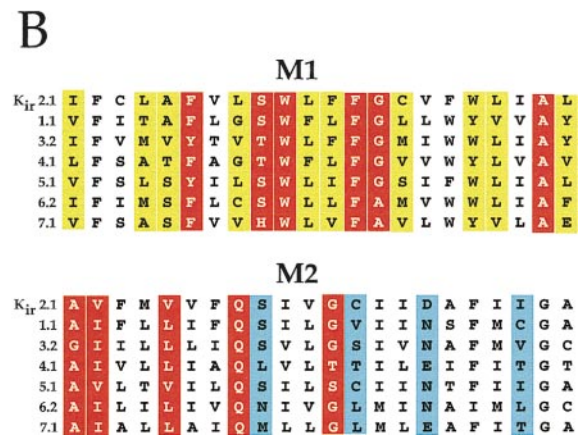

Figure 7. Arrangement of Transmembrane Helices in KcsA and K_{ir} 2.1 and Hallmark K_{ir} Sequence Patterns

(A) Schematic representation of the transmembrane helical arrangements in KcsA and K_{ir} 2.1 channels. In the KcsA arrangement, the M2 helices participate in subunit–subunit interactions, while the M1 helices interact only with M2 helices from their own subunit. In the K_{ir} arrangement, each M1 helix contacts two M2 helices, one via intrasubunit interactions and one via intersubunit interactions. M1 helices are colored orange and M2 helices yellow. The central green circle denotes a potassium ion in the pore of the channel.

(B) Hallmark sequence patterns in the transmembrane domains of K_{ir} superfamily members. Positions of restricted amino acid positions in K_{ir} 2.1 are indicated in red. Positions that face lipid (cf. Figure 5A) are colored yellow, and those that face the aqueous pore of the channel are colored blue (cf. Figure 5B). The hallmark patterns in M1 and M2 are $FX_2SWX_2FGX_6A$ and $A(V/I)X_2(V/L)X_2QX_3G$, respectively. Sequences are K_{ir} 2.1 residues 87–108 and 157–178 (Kubo et al., 1993), K_{ir} 1.1 residues 83–104 and 156–177 (Ho et al., 1993), K_{ir} 3.2 residues 97–118 and 169–190, K_{ir} 4.1 residues 70–91 and 143–164 (Takumi et al., 1995), K_{ir} 5.1 residues 76–97 and 146–167 (Bond et al., 1994), K_{ir} 6.2 residues 74–95 and 145–166 (Inagaki et al., 1995), and K_{ir} 7.1 residues 59–80 and 134–155 (Krapivinsky et al., 1998).

arrangements of these channels differ significantly. The M1 helices in K_{ir} channels are situated between two M2 helices where they may participate in subunit–subunit interactions (Figure 7A), while the M1 helices in KcsA only contact one M2 helix (Doyle et al., 1998). In K_{ir} channels, this difference may impact the location of determinants for subunit assembly and the placement of the pore helix and residues from the P region relative to the ion conduction pathway. However, these differences do not preclude an arrangement where the C-terminal end of the pore helix remains aimed at the ion conduction pathway.

Discussion

The information in the amino acid sequence that determines the final folded structure of a protein is highly degenerate, allowing many different sequence variations to encode for essentially the same structure. Selection of functional protein sequences from pools of related sequences allows one to examine the tolerance to change at each position within a given structural framework. In favorable circumstances, these types of investigations reveal positions of high and low information content, information about the local environment of each residue, and sets of interactions that are essential for establishing a specific protein fold (Bowie et al., 1990). For simple folds such as those that are common to membrane proteins, this information can lead to testable structural models for the transmembrane structure of a given protein.

There is a strong tendency for membrane-embedded polypeptides to form regular secondary structures in order to satisfy the maximal number of backbone hydrogen bonds (Popot and Engelman, 1990; von Heijne, 1997). However, beyond this feature, the "rules" for membrane protein folding are less well understood than those for soluble proteins. Uniquely packed structures are common in functional, soluble proteins (Richards and Lim, 1994). In contrast, well-packed specific structures (Lemmon et al., 1994; Bowie, 1997), as well as passively assembled structures of linked transmembrane helices (Lemmon and Engelman, 1994; Kaback et al., 1997; Zhou et al., 1997), have been reported in functional membrane proteins. The patterns of high and low information content positions in K_{ir} 2.1 clearly suggest that the transmembrane fold of the K_{ir} 2.1 channel has characteristics typical of a well-packed protein structure.

It has been suggested that K_{ir} channels may be structurally related to the last two transmembrane segments of the six transmembrane voltage-gated potassium channels (Jan and Jan, 1994). The structural differences between the topologically identical K_{ir} and KcsA potassium channels raise questions regarding which arrangement of helices is closer to the analogous structure in the voltage-gated channels. The sequence of KcsA is more similar to voltage-gated channels than K_{ir} channels (Schrempf et al., 1995; Doyle et al., 1998), and K_{ir} channels have sequence hallmarks that are not found in other potassium channels. These observations suggest that KcsA may more closely resemble the structure in the last two transmembrane segments of the voltage-gated channels, whereas the K_{ir} channels form a structurally distinct class.

A sequence alignment of representative members from each of the K_{ir} subfamilies (Figure 7B) shows that the pattern of restricted residues (red) identified in M1 of K_{ir} 2.1, $FX_2SWX_2FGX_6A$ is strongly conserved in all K_{ir} family members. Similarly, the pattern of restricted positions in M2, $A(V/I)X_2(V/L)X_2QX_3G$ is also strongly conserved. These patterns include the residues that participate in the putative membrane-embedded Ser95–

Gln164 hydrogen bond. The positions of high variability that comprise the lipid-facing (yellow) and pore-facing (blue) residues also seem to be well matched. The prevalence of these patterns within the K_{ir} superfamily suggests that these are hallmark sequence patterns reflecting the stereochemical requirements for building a structural framework shared by the transmembrane portions of all K_{ir} channels. Interestingly, some of the positions that appear strongly conserved in the sequence alignment (cf. F88 and G177) are extremely permissive to change in our selection experiments, indicating that conservation within related families of sequences does not always correspond to positions that are essential for function, at least when assayed in heterologous expression systems. The hallmark patterns identified here are absent in all other known potassium channels, including voltage-gated channels and the two P domain channels with parts that topologically resemble K_{ir} subunits (Ketchum et al., 1995; Lesage et al., 1996; Wei et al., 1996; Fink et al., 1998). These sequence comparisons add further support to the assertion that K_{ir} channels are structurally unique.

The P region sequence is the region of highest homology among potassium channels (Heginbotham et al., 1994), forms part of the ion conductance pathway, and contains the residues critical for ion selectivity. Data concerning the interaction of the P region sequence of voltage-gated potassium channels with the extracellular blockers tetraethylammonium (TEA) and channel-blocking peptide toxins are very well explained by the structure of this region in KcsA (Doyle et al., 1998) and suggest that this region is structurally similar in different potassium channel types (MacKinnon et al., 1998). The notable exception is the P region of K_{ir} channels. A single point mutation in the P region of a *Shaker* voltage-gated channel confers sensitivity to extracellular TEA block. This mutation has also been shown to bestow TEA sensitivity to a TEA-insensitive calcium-activated potassium channel (Ishii et al., 1997). However, this same mutation did not bestow TEA sensitivity when incorporated at the analogous position in TEA-insensitive K_{ir} channels (Bond et al., 1994).

Peptide toxins have been very useful for probing the features of the P region in voltage-gated channels (Miller, 1995). Until recently, there were no high-affinity peptide toxins for any K_{ir} channels (Jin and Lu, 1998), and a number of studies demonstrated that the high-affinity peptide toxins that interact so well with voltage-gated channels do not interact with K_{ir} channels as tightly or in the same way (Lu and MacKinnon, 1997; Imredy et al., 1998; Jin and Lu, 1998). Charybdotoxin family members share a conserved lysine that interacts directly with the potassium permeation pathway of voltage-gated channels (Park and Miller, 1992; Miller, 1995). Mutation of this lysine to alanine in three different toxin family members drastically alters the binding affinity ($>$1000-fold) for these channels. Recently, a toxin from this family, LQ2, has been found to interact with the inward rectifier K_{ir} 1.1 (Lu and MacKinnon, 1997). In contrast to its dramatic consequences for the binding affinity of the toxin for voltage-gated channels, the mutation of the pore-blocking conserved lysine to alanine has only modest effects ($\sim$10-fold) on the binding affinity of LQ2 for K_{ir} 1.1 (Lu and MacKinnon, 1997). Together, the findings with TEA and peptide toxin blockers suggest that structural differences exist between K_{ir} channels and other potassium channels in the region where potassium channels have the highest degree of sequence homology. This is consistent with the idea that K_{ir} channels are structurally different from other potassium channels. Since the P region bridges the M1 and M2 transmembrane helices of K_{ir} channels, the packing arrangement of M1 and M2 is expected to impact its structure. Thus, differences in the transmembrane structure are likely to be propagated to other parts of the ion conduction pathway.

Since the structural scaffold we have identified seems to be shared by all K_{ir} channels, the structural model presented here should provide a useful conceptual framework for pursuing detailed studies of the transmembrane segments in other K_{ir} potassium channels. For instance, it points to residues on the exterior surface of the M1 helices that may provide an interaction surface for membrane resident molecules such as auxiliary protein subunits (Babenko et al., 1998) or lipids (Baukrowitz et al., 1998; Huang et al., 1998; Shyng and Nichols, 1998; Sui et al., 1998) that regulate the function of some K_{ir} channels. Our results also uncover the structural complexity that can exist in a seemingly simple protein fold of a tetramer of subunits with two transmembrane helices each. Finally, the general approach outlined here provides a method for obtaining detailed structural information for transmembrane segments of potassium channels in the absence of high-resolution data.

Experimental Procedures

Library Construction

K_{ir} 2.1 was cloned into a derivative of pYES2 (Invitrogen) containing the following changes: the PvuI restriction site at position 2516 (pYES2 numbering) was destroyed by changing sequence 5′-GTAC GATCG-3′ to 5′-GTAGGATCG-3′ (change underlined), and the PvuI site at position 4417 was destroyed by changing sequence 5′-CAAC GATCGGAG-3′ to 5′-CAACGATTGGAG-3′ by single-strand mutagenesis. The gene for K_{ir} 2.1 (Kubo et al., 1993) was modified to remove the BglII site from residue 386 and to contain BglII, PvuI, and SfiI sites at amino acid residues 111, 142, and 177, respectively, and was cloned into the HindIII–XhoI sites of the vector. All gene changes preserve the wild-type amino acid sequence of K_{ir} 2.1 and create a construct in which the M1 and M2 regions were framed by BglII–SalI and PvuI–SfiI restriction sites, respectively. Finally, the GAL4 promotor was excised from the plasmid and replaced with the Met-25 promotor (Kerjan et al., 1986). K_{ir} 2.1-M1-stuffer and K_{ir} 2.1-M2-stuffer were made by cloning a cassette encoding nucleotides 210–1720 of the *Drosophila* protein Inscuteable (Kraut and Campos-Ortega, 1996) in frame into either the BglII–SalI or PvuI–SfiI sites. This was done to facilitate cloning and to ensure that simple plasmid religation in construction of the libraries resulted in nonfunctional K_{ir} 2.1 genes.

Cassettes for M1 and M2 were synthesized by PCR of overlapping oligonucleotides (Biosynthesis, Houston, TX) in which the bases for amino acid codons 87–108 and 157–178 contained 88% of the wild-type base and 4% each of the other three bases (Reidhaar-Olson et al., 1991). This yields an average of five codon changes per sequence. Cassettes were cloned into the appropriate K_{ir} 2.1-stuffer plasmid.

Selection

Selection experiments were conducted in the yeast strain SGY1528 (Mat***a*** *ade*2–1 *can*1–100 *his*3–11,15 *leu*2–3,112 *trp*1–1 *ura*3–1 *trk*1::HIS3 *trk*2::TRP1) (Tang et al., 1995). Libraries were transformed

into SGY1528 yeast and plated onto nonselective conditions containing 100 mM KCl. After 2 days of growth, the yeast were replica plated onto plates containing 1 mM KCl, allowed to grow for 2 days, and finally replica plated onto plates containing 0.5 mM KCl. All growth was at 30°C. Plasmids were rescued from K_{ir} 2.1 mutants that grew on 0.5 mM KCl plates, sequenced, and transformed a second time into SGY1528 to confirm the phenotype.

Nonselective plates were made from standard −ura/−met dropout media supplemented with 100 mM KCl and titrated to pH 6.5 with free Tris base. Selective plates contained the following components: −ura/−met dropout powder, 1.5% SeaKem LE agarose (FMC), 1 mM $MgSO_4$, 50 μM $CaCl_2$, 1% dextrose, 0.81 μM-H_3BO_3, 0.14 μM $Cu(II)SO_4{\cdot}(H_2O)$, 0.6 μM KI, 1.8 μM $Fe(II)SO_4{\cdot}(H_2O)_7$, 2.6 μM $MnSO_4$, 7.3 μM $(NH_4)_6Mo_7O_{24}$, 1.4 μM $ZnSO_4$, 8.1 nM biotin, 1.7 μM D-pantothenic acid hemicalcium salt, 3.2 μM nicotinic acid, 1.9 μM pyridoxine·HCl, 1.2 μM thiamine, and 11 μM inositol. Media was adjusted to pH 6.0 with H_3PO_4 and supplemented with either 1 mM or 0.5 mM KCl.

Periodicity Analysis

Power spectra of the amino acid variability of allowed substitutions in M1 and M2 were calculated using published algorithms (Cornette et al., 1987) (Professor D. R. Rees, CalTech). Discrete Fourier transform methods and least-squares methods gave the same principal peaks. The peak near $\omega = 170°$ in the M2 spectra is not seen using the least-squares procedure.

Electrophysiology

Constructs for electrophysiology were subcloned into a pGEMHE (Liman et al., 1992) derivative, and RNA transcripts were made using the Ampliscribe kit (Epicentre Technologies). Two-electrode voltage clamp experiments (CA-1; Dagan Instruments, Minneapolis) were made on defolliculated stage V–VI *Xenopus laevis* oocytes that had been microinjected with ~5–10 ng of RNA transcripts. Before injection, oocytes were surgically removed and treated with 2 mg/ml collagenase (Worthington) in 96 mM NaCl, 2 mM KCl, 1 mM $MgCl_2$, 5 mM HEPES (pH 7.5) at room temperature for 2 hr. Recordings were made 12–48 hr postinjection in a bath of either 90 K (90 mM KCl, 1 mM $MgCl_2$, 10 mM HEPES [pH 7.5]) or 90 Na (90 mM NaCl, 1 mM $MgCl_2$, 10 mM HEPES [pH 7.5]) solutions. Electrodes were filled with 3 M KCl and had resistances of 0.3–1.5 MΩ. Data were processed using PCLAMP software (Axon Instruments). For the subunit interaction assay, oocytes were injected with mixtures of K_{ir} 2.1-C+36 and wild-type K_{ir} 2.1 or S95E/Q164S RNA's at different ratios. Recordings were measured in a bath of 90 K or 90 Na solutions.

Structure Analysis

Nearest-neighbor contacts for KcsA were calculated from the Protein Data Bank coordinates (Doyle et al., 1998) using a program written by T. G. Oas (Oas and Kim, 1988). Nearest-neighbor van der Waals interactions were evaluated at ≤110% and ≤150% of the sum of the atom–atom van der Waals radii.

Acknowledgments

We thank members of the Jan lab for helpful input at all stages of this project. In particular, we thank B. Schwappach. We also thank Drs. S. Kurtz for the mutant yeast strain, R. MacKinnon for the KcsA coordinates, D. C. Rees for the power spectra programs, M. G. Oakley for figure assistance, P. A. B. Harbury for helpful advice, and C. I. Bargmann, J. U. Bowie, Z. Y. Peng, and N. Unwin for helpful comments on the manuscript. This study was supported by an NIH grant. Y. N. J. and L. Y. J. are HHMI investigators.

Received December 28, 1998; revised February 17, 1999.

References

Babenko, A.P., Aguilar-Bryan, L.A., and Bryan, J. (1998). A view of SUR/K_{ir} 6.X K_{ATP} channels. Annu. Rev. Physiol. *60*, 667–687.

Bargmann, C.I., and Weinberg, R.A. (1988). Oncogenic activation of the *neu*-encoded receptor protein by point mutation and deletion. EMBO J. *7*, 2043–2052.

Baukrowitz, T., Schulte, U., Oliver, D., Herlitze, S., Krauter, T., Tucker, S.J., Ruppersberg, J.P., and Fakler, B. (1998). PIP_2 and PIP as determinants for ATP inhibition of K_{ATP} channels. Science *282*, 1141–1144.

Bond, C.T., Pessia, M., Xia, X.M., Lagrutta, A., Kavanaugh, M.P., and Adelman, J.P. (1994). Cloning and expression of a family of inward rectifier potassium channels. Receptors Channels *2*, 183–191.

Bowie, J.U. (1997). Helix packing in membrane proteins. J. Mol. Biol. *272*, 780–789.

Bowie, J.U., Reidhaar-Olson, J.F., Lim, W.A., and Sauer, R.T. (1990). Deciphering the message in protein sequences: tolerance to amino acid substitutions. Science *247*, 1306–1310.

Cohen, C., and Parry, D.A.D. (1990). α-helical coiled coils and bundles: how to design an α-helical protein. Proteins *7*, 1–15.

Corey, S., Krapivinsky, G., Krapivinsky, L., and Clapham, D.E. (1998). Number and stoichiometry of subunits in the native atrial G-protein regulated K^+ channel I_{KACh}. J. Biol. Chem. *273*, 5271–5278.

Cornette, J.L., Cease, K.B., Margarlit, H., Spouge, J.L., Berzofsky, J.A., and DeLisi, C. (1987). Hydrophobicity scales and computational techniques for detecting amphipathic structures in proteins. J. Mol. Biol. *195*, 659–685.

Donnelly, D., Overington, J.P., Ruffle, S.V., Nugent, J.H.A., and Blundell, T.L. (1993). Modelling α-helical transmembrane domains: the calculation and use of substitution tables for lipid-facing residues. Protein Sci. *2*, 55–70.

Doupnik, C.A., Davidson, N., and Lester, H.A. (1995). The inward rectifier potassium channel family. Curr. Opin. Neurobiol. *5*, 268–277.

Doyle, D.A., Cabral, J.M., Pfuetzner, R.A., Kuo, A., Gulbis, J.M., Cohen, S.L., Chait, B.T., and MacKinnon, R. (1998). The structure of the potassium channel: molecular basis of K^+ conduction and selectivity. Science *280*, 69–77.

Fink, M., Lesage, F., Duprat, F., Heurteaux, C., Reyes, R., Fosset, M., and Lazdunski, M. (1998). A neuronal two P domain K^+ channel stimulated by arachidonic acid and polyunsaturated fatty acids. EMBO J. *17*, 3297–3308.

Heginbotham, L., Lu, Z., Abramson, T., and MacKinnon, R. (1994). Mutations in the K^+ channel signature sequence. Biophys. J. *66*, 1061–1067.

Hille, B. (1992). Ionic Channels of Excitable Membranes. (Sunderland, MA: Sinauer Associates, Inc.).

Ho, K., Nichols, C.G., Lederer, W.J., Lytton, J., Vassilev, P.M., Kanazirska, M.V., and Hebert, S.C. (1993). Cloning and expression of an inwardly rectifying ATP-regulated potassium channel. Nature *362*, 31–38.

Huang, C.L., Feng, S., and Hilgemann, D.W. (1998). Direct activation of inward rectifier potassium channels by PIP_2 and its stabilization by Gβγ. Nature *391*, 803–806.

Hubbell, W.L., Gross, A., Langen, R., and Lietzow, M.A. (1998). Recent advances in site-directed spin labeling of proteins. Curr. Opin. Struct. Biol. *8*, 649–656.

Imredy, J.P., Chen, C., and MacKinnon, R. (1998). A snake toxin inhibitor of inward rectifier potassium channel ROMK1. Biochemistry *37*, 14867–14874.

Inagaki, N., Gonoi, T., Clement, J.P., IV, Namba, N., Inazawa, J., Gonzalez, G., Aguilar-Bryan, L., Seino, S., and Bryan, J. (1995). Reconstitution of I_{KATP}: an inward rectifier subunit plus the sulfonylurea receptor. Science *270*, 1166–1170.

Ishii, T.M., Maylie, J., and Adelman, J.P. (1997). Determinants of apamin and *d*-tubocurarine block in SK potassium channels. J. Biol. Chem. *37*, 23195–23200.

Jan, L.Y., and Jan, Y.N. (1994). Potassium channels and their evolving gates. Nature *371*, 119–122.

Jan, L.Y., and Jan, Y.N. (1997). Cloned potassium channels from eukaryotes and prokaryotes. Annu. Rev. Neurosci. *20*, 91–123.

Jin, W., and Lu, Z. (1998). A novel high-affinity inhibitor for inward-rectifier K^+ channels. Biochemistry *37*, 13291–13299.

Kaback, H.R., Voss, J., and Wu, J. (1997). Helix packing in polytopic membrane proteins: the lactose permease of *Escherichia coli*. Curr. Opin. Struct. Biol. *7*, 537–542.

Kerjan, P., Surdin-Kerjan, Y., and Cherest, H., (1986). Nucleotide sequence of the *Saccharomyces cerevisiae* MET25 gene. Nucleic Acids Res. *14*, 7861–7871.

Ketchum, K.A., Joiner, W.J., Sellers, A.J., Kaczmarek, L.K., and Goldstein, S.A.N. (1995). A new family of outwardly rectifying potassium channel proteins with two pore domains in tandem. Nature *376*, 690–695.

Krapivinsky, G., Medina, I., Eng, L., Krapivinsky, L., Yang, Y., and Clapham, D.E. (1998). A novel inward rectifier K^+ channel with unique pore properties. Neuron *20*, 995–1005.

Kraut, R., and Campos-Ortega, J.A. (1996). Inscuteable, a neural precursor gene of Drosophila, encodes a candidate for a cytoskeleton adaptor protein. Dev. Biol. *174*, 65–81.

Kubo, Y., Baldwin, T.J., Jan, Y.N., and Jan, L.Y. (1993). Primary structure and functional expression of a mouse inward rectifier potassium channel. Nature *362*, 127–133.

Lemmon, M.A., and Engelman, D.M. (1992). Helix-helix interactions inside lipid bilayers. Curr. Opin. Struct. Biol. *2*, 511–518.

Lemmon, M.A., and Engelman, D.M. (1994). Specificity and promiscuity in membrane helix interactions. Q. Rev. Biophys. *27*, 157–218.

Lemmon, M.A., Flanagan, J.M., Treutlein, H.R., Zhang, J., and Engelman, D.M. (1992). Sequence specificity in the dimerization of transmembrane α-helices. Biochemistry *31*, 12719–12725.

Lemmon, M.A., Treutlein, H.R., Adams, P.D., Brünger, A.T., and Engelman, D.M. (1994). A dimerization motif for transmembrane α-helices. Nat. Struct. Biol. *1*, 157–163.

Lesage, F., Guillemare, E., Fink, M., Duprat, F., Lazdunski, M., Romey, G., and Barhanin, J. (1996). A pH-sensitive yeast outward rectifier K^+ channel with two pore domains and novel gating properties. J. Biol. Chem. *271*, 4183–4187.

Liman, E.R., Tytgat, J., and Hess, P. (1992). Subunit stoichiometry of a mammalian K^+ channel determined by construction of multimeric cDNAs. Neuron *9*, 861–871.

Lu, Z., and MacKinnon, R. (1994). Electrostatic tuning of Mg^{2+} affinity in an inward-rectifier K^+ channel. Nature *371*, 243–246.

Lu, Z., and MacKinnon, R. (1997). Purification, characterization and synthesis of an inward rectifier K^+ channel inhibitor from scorpion venom. Biochemistry *36*, 6936–6940.

Lumb, K.J., and Kim, P.S. (1995). A buried polar interaction imparts structural uniqueness in a designed heterodimeric coiled coil. Biochemistry *34*, 8642–8648.

Lüscher, C., Jan, L.Y., Stoffel, M., Malenka, R.C., and Nicoll, R.A. (1997). G protein-coupled inwardly rectifying K^+ channels (GIRKs) mediate postsynaptic but not presynaptic transmitter actions in hippocampal neurons. Neuron *19*, 687–695.

MacKinnon, R., Cohen, S.L., Kuo, A., Lee, A., and Chait, B.T. (1998). Structural conservation in prokaryotic and eukaryotic potassium channels. Science *280*, 106–107.

Miller, C. (1995). The charybdotoxin family of K^+ channel-blocking peptides. Neuron *15*, 5–10.

Nestorowicz, A., Inagaki, N., Gonoi, T., Schoor, K.P., Wilson, B.A., Glaser, B., Landau, H., Stanley, C.A., Thornton, P.S., Seino, S., and Permutt, M.A. (1997). A nonsense mutation in the inward rectifier potassium channel gene, *Kir*6.2, is associated with familial hyperinsulinism. Diabetes *46*, 1743–1748.

Nichols, C.G., and Lopatin, A.N. (1997). Inward rectifier potassium channels. Annu. Rev. Physiol. *59*, 171–191.

Oas, T.G., and Kim, P.S. (1988). A peptide model of a protein folding intermediate. Nature *336*, 42–48.

Park, C.-S., and Miller, C. (1992). Mapping function to structure in a channel blocking peptide: electrostatic mutants of charybdotoxin. Biochemistry *31*, 7749–7755.

Perozo, E., Cortes, D.M., and Cuello, L.G. (1998). Three dimensional architecture and gating mechanism of a K^+ channel studied by EPR spectroscopy. Nat. Struct. Biol. *5*, 459–469.

Popot, J.-L., and Engelman, D.M. (1990). Membrane protein folding and oligomerization: the two-stage model. Biochemistry *29*, 4031–4037.

Raab-Graham, K.F., and Vandenberg, C.A. (1998). Tetrameric subunit structure of the native brain inwardly rectifying potassium channel K_{ir} 2.2. J. Biol. Chem. *273*, 19699–19707.

Rees, D.C., DeAntonio, L., and Eisenberg, D. (1990). Hydrophobic organization of membrane proteins. Science *245*, 510–513.

Reidhaar-Olson, J.F., Bowie, J.U., Breyer, R.M., Hu, J.C., Knight, K.L., Lim, W.A., Mossing, M.C., Parsell, D.A., Shoemaker, K.R., and Saver, R.T. (1991). Random mutagenesis of protein sequences using oligonucleotide cassettes. Methods Enzymol. *208*, 564–586.

Reuveney, E., Jan, Y.N., and Jan, L.Y. (1996). Contributions of a negatively charged residue in the hydrophobic domain of IRK1 inwardly rectifying K^+ channel to K^+-selective permeation. Biophys. J. *70*, 754–761.

Richards, F.M., and Lim, W.A. (1994). An analysis of packing in the protein folding problem. Q. Rev. Biophys. *26*, 423–498.

Sahin-Tóth, M., Dunten, R.L., Gonzalez, A., and Kabeck, H.R. (1992). Functional interactions between putative intramembrane charged residues in the lactose permease of *Escherichia coli*. Proc. Natl. Acad. Sci. USA *89*, 10547–10551.

Schrempf, H., Schmidt, O., Kummerlen, R., Hinnah, S., Muller, D., Betzler, M., Steinkamp, T., and Wagner, R. (1995). A prokaryotic potassium ion channel with two predicted transmembrane segments from *Streptomyces lividans*. EMBO J. *14*, 5170–5178.

Shyng, S.-L., and Nichols, C.G. (1998). Membrane phospholipid control of nucleotide sensitivity of K_{ATP} channels. Science *282*, 1138–1144.

Simon, D.B., Karet, F.E., Rodriguez-Soriano, J., Hamdan, J.H., DiPietro, A., Trachtman, H., Sanjad, S.A., and Lifton, R.P. (1996). Genetic heterogeneity of Bartter's syndrome revealed by mutations in the K^+ channel, ROMK. Nat. Genet. *14*, 152–156.

Smith, S.O., Smith, C.S., and Bormann, B.J. (1996). Strong hydrogen bonding interactions involving a buried glutamic acid in the transmembrane sequence of the neu/erbB-2 receptor. Nat. Struct. Biol. *3*, 252–258.

Stanfield, P.R., Davies, N.W., Shelton, P.A., Sutcliffe, M.J., Khan, I.A., Brammar, W.J., and Conley, E.C. (1994). A single aspartate residue is involved in both intrinsic gating and blockage by Mg^{2+} of the inward rectifier IRK1. J. Physiol. *478*, 1–6.

Sui, J.L., Petit-Jacques, J., and Logothetis, D. (1998). Activation of the atrial K_{ACh} channel by the $\beta\gamma$ subunits of G proteins or intracellular Na^+ ions depends on the presence of phosphatidylinositol phosphates. Proc. Natl. Acad. Sci. USA *95*, 1307–1312.

Takumi, T., Ishii, T., Horio, Y., Morishige, K., Takahashi, N., Yamada, M., Yamashita, T., Kiyama, H., Sohmiya, H., Nakanishi, S., et al. (1995). A novel ATP-dependent inward rectifier potassium channel expressed predominantly in glial cells. J. Biol. Chem. *270*, 16339–16346.

Tang, W., Ruknudin, A., Yang, W.P., Shaw, S.Y., Knickerbocker, A., and Kurtz, S. (1995). Functional expression of a vertebrate inwardly rectifying K^+ channel in yeast. Mol. Biol. Cell *6*, 1231–1240.

von Heijne, G. (1997). Principles of membrane protein assembly and structure. Prog. Biophys. Mol. Biol. *66*, 113–139.

Wallin, E., Tsukihara, T., Yoshikawa, S., von Heijne, G., and Elofsson, A. (1997). Architecture of helix bundle membrane proteins: an analysis of cytochrome *c* oxidase from bovine mitochondria. Protein Sci. *6*, 808–815.

Wei, A., Jegla, T., and Salkoff, L. (1996). Eight potassium channel families revealed by the *C. elegans* genome project. Neuropharmacology *35*, 805–829.

Wen, J., Chen, X., and Bowie, J.U. (1996). Exploring the allowed sequence space of a membrane protein. Nat. Struct. Biol. *3*, 141–148.

Wible, B.A., Taglialatela, M., Ficker, E., and Brown, A.M. (1994). Gating of inwardly rectifying K^+ channels localized to a single negatively charged residue. Nature *371*, 246–249.

Wickman, K.D., and Clapham, D.E. (1995). G-protein regulation of ion channels. Curr. Opin. Neurobiol. *5*, 278–285.

Yang, J., Jan, Y.N., and Jan, L.Y. (1995). Determination of the subunit stoichiometry of an inwardly rectifying potassium channel. Neuron *15*, 1441–1447.

Zerangue, N., Schwappach, B., Jan, Y.N., and Jan, L.Y. (1999). The stoichiometry of plasma membrane K_{ATP} channels is regulated by a new ER trafficking signal. Neuron, in press.

Zhou, Y., Wen, J., and Bowie, J.U. (1997). A passive transmembrane helix. Nat. Struct. Biol. *4*, 986–990.